2015-06-06

Mycolic acids, a promising mycobacterial ligand for targeting of nanoencapsulated drugs in tuberculosis

Lemmer, Yolandy

Elsevier

http://dx.doi.org/10.1016/j.jconrel.2015.06.005

Journal of Controlled Release 211 (2015) 94–104

Contents lists available at ScienceDirect

Journal of Controlled Release

journal homepage: www.elsevier.com/locate/jconrel

Mycolic acids, a promising mycobacterial ligand for targeting of nanoencapsulated drugs in tuberculosis

Yolandy Lemmer [a,*], Lonji Kalombo [a], Ray-Dean Pietersen [b], Arwyn T. Jones [c], Boitumelo Semete-Makokotlela [a], Sandra Van Wyngaardt [d], Bathabile Ramalapa [a], Anton C. Stoltz [e], Bienyameen Baker [b], Jan A. Verschoor [d], Hulda S. Swai [a], Chantal de Chastellier [f]

[a] Polymers and Composites, Council for Scientific and Industrial Research, Pretoria, South Africa
[b] DST-CBTBR Department Molecular Biology and Human Genetics, Stellenbosch University, Cape Town, South Africa
[c] Cardiff School of Pharmacy and Pharmaceutical Sciences, Cardiff University, Wales, UK
[d] Department of Biochemistry, University of Pretoria, Pretoria, South Africa
[e] Department of Infectious Diseases, University of Pretoria, Pretoria, South Africa
[f] Centre d'Immunologie de Marseille-Luminy (CIML), Aix Marseille University, UM 2, INSERM UMR 1104, CNRS UMR 7280, 163 avenue de Luminy, 13288 Marseille Cedex 09, France

ARTICLE INFO

Article history:
Received 5 March 2015
Received in revised form 2 June 2015
Accepted 4 June 2015
Available online 6 June 2015

Keywords:
Tuberculosis
Mycolic acids
Nanodrug delivery
Targeting
Phagosomes
Electron microscopy

ABSTRACT

The appearance of drug-resistant strains of *Mycobacterium tuberculosis* (*Mtb*) poses a great challenge to the development of novel treatment programmes to combat tuberculosis. Since innovative nanotechnologies might alleviate the limitations of current therapies, we have designed a new nanoformulation for use as an anti-TB drug delivery system. It consists of incorporating mycobacterial cell wall mycolic acids (MA) as targeting ligands into a drug-encapsulating Poly DL-lactic-co-glycolic acid polymer (PLGA), via a double emulsion solvent evaporation technique. Bone marrow-derived mouse macrophages, either uninfected or infected with different mycobacterial strains (*Mycobacterium avium*, *Mycobacterium bovis* BCG or *Mtb*), were exposed to encapsulated isoniazid-PLGA nanoparticles (NPs) using MA as a targeting ligand. The fate of the NPs was monitored by electron microscopy. Our study showed that i) the inclusion of MA in the nanoformulations resulted in their expression on the outer surface and a significant increase in phagocytic uptake of the NPs; ii) nanoparticle-containing phagosomes were rapidly processed into phagolysosomes, whether MA had been included or not; and iii) nanoparticle-containing phagolysosomes did not fuse with non-matured mycobacterium-containing phagosomes, but fusion events with mycobacterium-containing phagolysosomes were clearly observed.

1. Introduction

Tuberculosis (TB) is mainly a burden of the developing world, but has also a great impact globally with an estimated annual 8.6 million incident cases. It also ranks as the second leading cause of death from a communicable disease (second to Acquired Immunodeficiency Syndrome (AIDS)) with 1.3 million deaths reported in 2012 [1]. TB-AIDS can be classified as a new combination disease, since Human Immunodeficiency Virus/*Mycobacterium tuberculosis* (HIV/*Mtb*) co-infection has become such a frequent occurrence in third world countries. In comparison to TB alone, TB/AIDS patients have severely reduced survival times, are more challenging to diagnose [2] and may exhibit sometimes fatal immune reconstitution inflammatory syndrome (IRIS) when subjected to anti-retroviral therapy [3]. Standard first line chemotherapy is not effective for individuals that are infected with multi-drug resistant (MDR) *Mtb* strains and there is practically no cure for extensively-drug resistant (XDR) ones. Failure to complete the lengthy drug regimens allows the pathogens to become resistant especially to the two first line drugs, isoniazid (INH) and rifampicin (RIF). This is increasingly evident in persons who have been previously treated for TB [4]. It is now imperative to discover new chemotherapies against this mycobacterium as well as to enhance the efficacy of existing drugs to combat MDR and XDR forms [5]. In addition, it is important to find new technologies for targeting chemotherapeutic agents and toxic host cell effector molecules through the lipid-rich wax-like mycobacterial cell wall [6].

Innovative nanotechnologies have been designed and tested to meet the challenges posed by the pathogen and poor drug efficacy. Their potential to improve compliance, efficacy and affordability of therapy makes them especially suited for addressing the treatment of TB and AIDS. Nanomedicine (the medical application of nanotechnology) has the potential to improve bioavailability, reduce toxic side effects, reduce drug–drug interactions and overcome drug resistance. Furthermore, nanoformulations can improve drug solubility and facilitate

* Corresponding author at: CSIR, Material Science and Manufacturing, Meiring Naude Road, Bldg 14f, Brummeria, Pretoria 0001, South Africa.
E-mail address: ylemmer@csir.co.za (Y. Lemmer).

http://dx.doi.org/10.1016/j.jconrel.2015.06.005
0168-3659/

intracellular drug delivery as well as target drugs to the site of infection. Nano drug delivery systems are generally prepared with natural or synthetic compounds (i.e. polymers and lipids) using various techniques to yield particles ranging in size between 10 and 1000 nm in diameter [7]. Many groups have used poly DL, lactic–co-glycolic acid (PLGA) as the polymeric encapsulating material because it is non-immunogenic, biodegradable and has the capacity to encapsulate hydrophobic and hydrophilic agents [8]. PLGA was also shown to be selectively taken up into macrophages and dendritic cells [9], the main targets for infection with *Mtb* [10]. In addition, the cytotoxicity of PLGA was evaluated in vitro and in vivo and no significant adverse effects were noted [11].

Nanoencapsulation of drugs for delivery provides an opportunity to incorporate targeting strategies to further enhance drug efficiency and limit systemic toxic side-effects to the patient. By functionalizing the surface of the particles with a targeting ligand, higher bioavailability could be generated at the site of infection and therefore the dose and side effects of the drug are minimized [12]. An effective targeting strategy will impact positively on drug delivery to the site of infection, may direct the trafficking of the drugs into organelles in which pathogens are harboured and may improve the release and longevity of the active drug. A comprehensive review of the recent advances in targeting with drug carrier designs for TB was done by Dube and colleagues [13].

The mycobacterial cell wall is composed of many compounds that could serve as targeting ligands. Among these, mycolic acids (MA) are promising candidates because they are the dominant lipids found in the outer cell wall envelope of *Mycobacterium* species [14]. MA are long 2-alkyl 3-hydroxyl fatty acids and in *Mtb*, MA consist mainly of alpha-, keto- and methoxy classes, typically 70–90 carbon atoms in length, each containing mixtures of homologs of varying chain lengths and, in some cases different stereochemistry around functional groups in the main (mero-) chain [15]. The various subtypes of MA have been shown to play a major role in the virulence of the pathogen [6,16]. MA from *Mtb* have interesting biological activities, including foam cell formation and immune steering towards Th1 cellular responses [17–19], as well as cholesteroid like properties [20,21]. MA was also shown to be immunogenic. When presented by CD1b molecules on dendritic cells, proliferation of human $CD4^-$, $CD8^-$ (double negative) T-lymphocytes occurs [22,23]. In addition, anti-MA antibodies are found in human TB-positive patient serum [24]. Mycobacterial MA has never been tested as a ligand for improving nanoencapsulated antituberculosis (anti-TB) drug targeting. An attractive hypothesis would be that the MA present on the external surface of the NPs may interact with anti-MA antibodies in the vicinity of the sites of infection to cause a localised immune complex that may enhance uptake of the NPs in the infected and surrounding uninfected macrophages. MA could also target cholesterol present in the plasma membrane of uninfected or infected macrophages [25,26] and, more interestingly, in the membrane of phagosomes in which pathogenic mycobacteria are harboured [27], by means of its attraction to cholesterol [20,21,28].

To understand whether or how this happens demands an intricate knowledge of the cellular and molecular mechanisms of survival of the pathogen of interest and more precisely how the pathogen uses or diverts the cellular machinery to its advantage. It is well known that the preferred site of residence of pathogenic mycobacteria in the host macrophage is the immature phagosome [29] which is unable to fuse with lysosomes [30,31]. However, mycobacteria internalized in clumps, a frequent event in the case of *Mtb*, are unable to block phagosome maturation [32–35]. In this case, phagosomes mature and fuse with lysosomes to become phagolysosomes. Interestingly, mycobacteria do not die in this cytolytic environment from which they are eventually rescued to reside in phagosomes that no longer fuse with lysosomes [29]. Several more recent studies also indicate that *Mtb*, but not *Mycobacterim bovis* BCG or *Mycobacterium avium*, may evade phagosomes to survive in the host cell cytosol immediately prior to host cell lysis [36–39].

The subcellular localisation of PLGA particles in cells is a field that has hitherto yielded conflicting results over the past decade. On the one hand, PLGA particles were suggested to be able to escape the endomembrane compartments into the cytosol of a smooth muscle cell line within minutes after phagocytic uptake [12,40]. More groups supported this interpretation for different cell types, including macrophages [41–43]. On the other hand, the PLGA particles were suggested to remain within the phagolysosomal compartment for several days [44–46]. Another issue is the ability for PLGA particles to reach the compartment in which mycobacteria reside. One group suggested this possibility [47], but others could not demonstrate it [10,45].

Previous efforts to demonstrate a potential benefit of MA as a drug-targeting ligand utilized fluorescently labelled MA in a human myelomonocytic cell line by means of confocal laser-scanning fluorescence microscopy (CLSM) [48]. The fluorescently labelled MA in NPs were shown to be actively taken up by the cell lines. In the present work, we assess the use of mycobacterial MA as a ligand for nanoencapsulated anti-*Mtb* drug targeting on the uptake and intracellular fate of the NPs by electron microscopy (EM) methods. It is important to recall that EM is the only technique that can combine sensitive protein detection methods with detailed information on the ultrastructure and interaction of mycobacteria and cellular compartments. A nanoformulation of incorporated MA in a PLGA polymer was achieved via the double emulsion solvent evaporation technique. INH was incorporated as the anti-TB drug model in our PLGA particles due to its known cytotoxicity as a first line drug against actively replicating *Mtb*. We chose to infect mouse bone marrow-derived macrophages (BMDM) with either *Mtb*, *M. bovis* BCG or *M. avium*. Six days later, cells were exposed to the synthesized NPs, with or without the potential targeting ligand MA. We show that MA enhanced the uptake of NPs into mycobacterium-infected macrophages. Newly formed nanoparticle-containing phagosomes were processed into phagolysosomes within hours. Such phagolysosomes were able to fuse with and deliver their contents to mycobacterium-containing phagolysosomes but not to immature phagosomes. We now clearly demonstrate that NPs do co-localise with mycobacteria in the phagolysosomal compartments.

2. Materials and methods

2.1. Chemicals and reagents

Dimethyl sulfoxide, Isoniazid (99%), mycobacteria-derived MA, PLGA 50:50 (Mw: 45,000–75,000), Polyvinyl alcohol MW: 13,000–2,3000 partially hydrolysed (87–89%), Sodium dodecyl sulphate, Triton X-100, Trypan blue, Basic fuchsin, Dulbecco's modified Eagle's medium (DMEM), Tyloxapol and Glutaraldehyde grade I (EM grade) were purchased from Sigma-Aldrich Chemical Co., (St Louis, MO, USA). Foetal bovine serum (FBS) was from Biowest (Nuaillé, France), phosphate-buffered saline (PBS) was from GIBCO (distributed by Invitrogen, Villebonsur Yvette, France), and osmium tetroxide and Spurr resin were from Electron Microscopy Sciences (distributed by Euromedex, Mundolsheim, France). Middlebrook 7H9, 7H10 agar and Oleic acid-albumin-dextrose-catalase (OADC) were from Difco Inc. (Detroit, MI, USA). Bovine serum albumin conjugated to gold particles (BSA-Au) was purchased from the Utrecht University School of Medicine (Utrecht, The Netherlands).

2.2. Preparation of NPs

The double emulsion solvent evaporation freeze drying technique was used as previously described with modifications [49]. PLGA 50:50 (MW: 45,000–75,000) was dissolved in 6 ml of dichloromethane (DCM) at a concentration of 1.25% weight/volume (w/v). For particles containing MA, isolated MA from *Mtb* (2 mg, 1.7 μmol) was dissolved in 2 ml DCM and added while stirring. For the first water-in-oil (w/o) emulsion, 2 ml of aqueous PBS, pH 7.4, was added to the mixture and homogenized at 5000 rpm for 3 min in a bench-top homogenizer at 4 °C. For NPs containing INH, INH (100 mg, 729 μmol) was dissolved

in PBS and then added to the mixture. The emulsion formed was subsequently transferred to an aqueous stabilizer solution of 2% (w/v) polyvinyl alcohol. The second water-in-oil-in-water (w/o/w) emulsion was formed by homogenization at 8000 rpm for 7 min, then stirred at 500 rpm overnight at atmospheric pressure and room temperature to evaporate the organic solvent. The PLGA NPs were recovered by centrifugation at 845 and 33,902 rcf respectively for 15 min. The resulting particles were dried by lyophilization in a Virtis Benchtop freeze dryer.

2.3. Nanoparticle characterisation

NPs collected after lyophilization were subjected to size and size distribution (polydispersity index) measurements by means of dynamic light scattering as well as surface potential measurements by means of laser doppler electrophoresis using a Zetasizer NanoZS instrument (Malvern Instruments ltd. UK). NPs were also deposited onto aluminium stubs and coated with carbon in a glow-discharge apparatus to examine their surface morphology by scanning electron microscopy (SEM).

2.4. Quantification of INH and MA within NPs

Quantification of the INH encapsulated in the NPs was performed via the direct method. Lyophilized NPs (10.0 mg) were suspended in 10 ml 0.05 M NaOH and kept at room temperature (RT) overnight with continuous agitation. The samples were then neutralised with 0.1 M HCl and analyzed via UV spectrometry at 260 nm [50].

Carbolfuchsin dye was used to quantify the amount of MA present in the NPs [51]. The MA-containing NPs (20.0 mg) were dissolved in chloroform (10 ml) and stirred overnight. Hexane was added to precipitate the PLGA, and stirred vigorously for an hour. The precipitate was recovered by filtration through a 0.45 μm organic solvent resistant filter (Pall Acrodisk) and washed two to three times with hexane. The hexane extract was evaporated with nitrogen gas. The MA left in the vial was re-dissolved in hexane (1 ml) followed by the addition of an equal amount of carbolfuchsin dye. The absorbance of the hexane layer was measured at 492 nm in an absorbance plate reader and a standard curve was compiled.

2.5. Immuno detection of MA on particle surfaces

The presence of MA on the surface was confirmed by Enzyme-linked immunosorbent assay (ELISA). Preparation of the ELISA plates was done as previously described with modifications [28,52,53]. Where liposomes were used in the inhibition of serum anti-MA antibodies in literature (75 μg MA/1 μl of serum), we used MA-NPs (2 μg MA/1 μl of serum). MA for coating of the ELISA plates was prepared by dissolving the lipid in hexane (3 μg/50 μl), vortexing for one minute, heating at ~85 ° C for 1 min and left to stand at room temperature for 15 min. Hexane without MA served as coating control. The ELISA plates were coated with the MA at 50 μl per well using a Hamilton syringe. Plates were stored in a plastic bag at 4 °C overnight. The coated plates were blocked with 0.5% Casein/PBS pH 7.4 (400 μl/well) at RT. After 2 h, the blocking buffer was aspirated and serum (1:20 dilution in 0.5% Casein/PBS, pH7.4) was added to the plate (50 μl/well). Before the TB positive and negative human sera were added to the wells, the serum was incubated for 1 h with PLGA NPs with or without MA (2 mg/ml). Human sera used for analysis of NPs were from a TB-positive patient serum and a healthy control, both collected by Anton Stoltz of the Department of Internal Medicine (Infectious Diseases), Faculty of Health Sciences, University of Pretoria and were approved by the University Ethics Committee (159/2011 of 1 September 2011). Samples were centrifuged to remove particulate material and the supernatant was added to the plates (50 μl/well). After 1 h of incubation, the wells were washed three times with a Well Wash4 ELISA washer (Labsystems). The wells were then exposed to goat anti-human Immunoglobulin G (H + L) peroxidase conjugate (50 μl/well) for 30 min. at RT. After the incubation the wells were washed three times with Casein/PBS, then incubated at RT with 50 μl per well of the substrate solution consisting of 10 mg of OPD plus 8 mg of Urea–H_2O_2 in 10 ml of citrate buffer to develop the peroxidase activity. After 30 min, the plate was read with a SLT 340 ATC photometer at 450 nm with a reference filter at 690 nm. Background binding of the serum to the plate was corrected for by subtracting the average binding signal of serum to MA from that registered for the hexane coated wells. Statistical comparisons of ELISA results were performed using the student t-test at a confidence level of 95%.

2.6. Mycobacteria

Three different mycobacterial strains were used: i) *M. avium*. The transparent colony variant TMC 724 (serovar 2) was prepared as earlier described [32]. Briefly, mycobacteria of a first passage were expanded after isolation from the liver of C57BL/6 mice infected 6–8 weeks previously. Mycobacteria used for experiments were always of the first passage grown on Middlebrook 7H10 agar plates, supplemented with 0.5% Tween 80, 0.2% glycerol and 10% OADC; ii) *M. bovis* BCG Pasteur 1173P2 was grown in Sauton's medium containing 0.05% tyloxapol; iii) *Mtb* H37Rv was grown in Middlebrook 7H9 supplemented with 0.5% Tween 80, 0.2% glycerol and 10% OADC. For all three strains, aliquots of bacterial suspensions were concentrated in Middlebrook 7H9 medium devoid of Tween and stored at −80 °C. When required, frozen samples were quickly thawed, vortexed and adjusted to the desired titre in complete cell culture medium. At least 90% of the mycobacteria were morphologically intact and viable at this stage.

2.7. Cell culturing and phagocytic uptake

Bone marrow cells were isolated from femurs of 6- to 8-week-old C57BL/6 female mice and seeded onto tissue culture dishes (Falcon, Becton Dickinson Labware, Meylan, France) of 35 mm in diameter (4×10^5 cells per dish) or on 24-well tissue culture plates (1×10^5 per well). The culture medium was Dulbecco's modified Eagle's medium (DMEM) with high glucose (1 g/L) and high carbonate (3.7 g/L) concentrations supplemented with 10% heat-inactivated foetal bovine serum (FBS), 10% L-cell conditioned medium (a source of CSF-1), and 2 mM L-glutamine. At 5 days after seeding, the adherent cells were washed twice with DMEM and re-fed with complete medium. Medium was then renewed on day 6. No antibiotics were added. Seven-day-old macrophages were infected for 4 h at 37 °C with either *M. avium* at a Multiplicity of Infection (MOI) of 20, *M. bovis* BCG at a MOI of 5, or *Mtb* at a MOI of 2. Infected cells were washed in four changes of ice-cold PBS to eliminate non-ingested bacteria, and further incubated in complete medium devoid of antibiotics.

2.8. Treatment with NPs and chase in NP-free medium

After active replication of mycobacteria for 6 days, infected cells were exposed to INH-encapsulated PLGA NPs (0.1 mg per ml of medium), with or without the targeting ligand, MA, for 2–4 h. Cells were washed gently with three successive changes of DMEM and re-incubated in complete medium devoid of NPs. At selected time points post-treatment (0–12 days), cells were fixed and processed for EM as described below. Cells remained 98% viable for the entire duration of the experiment, irrespective of post-infection treatment (data not shown).

2.9. Labelling of lysosomes with BSA-gold

To label lysosomes, *M. bovis BCG*-infected macrophages were rinsed with serum-free medium and incubated for 30 min at 37 °C with colloidal gold particles of 10 nm in diameter conjugated with bovine serum

albumin (BSA-Au) diluted in serum-free medium. Cells were washed three times with serum-free medium and further incubated in complete medium devoid of BSA-Au for 2 h at 37 °C. BSA-Au-treated cells were then exposed to NPs as described above. At selected time points during the treatment or the chase period, cells were fixed and processed for EM. Nanoparticle-containing phagosomes were examined for the presence or absence of BSA-Au.

2.10. Processing for conventional EM

Cells were fixed for 1 h at RT with 2.5% glutaraldehyde in 0.1 M Na-cacodylate buffer, pH 7.2, containing 0.1 M sucrose, 5 mM $CaCl_2$ and 5 mM $MgCl_2$. After this, they were washed with complete cacodylate buffer, and post-fixed for 1 h at RT with 1% osmium tetroxide in the same buffer, but devoid of sucrose. Cells were then washed with buffer, scraped off the dishes, concentrated in 2% agar in cacodylate buffer and treated for 1 h at RT with 1% uranyl acetate in 30% methanol. Samples were dehydrated in a graded series of ethanol and embedded in Spurr resin. Thin sections (70 nm-thick) were stained with 1% uranyl acetate in distilled water and then with lead citrate.

2.11. Quantifications

At the time points indicated, 100 to 200 different cell profiles were examined under the EM to determine the number of NPs per cell profile. Nanoparticle-containing cell profiles were then examined to determine the percentage of NPs enclosed in phagolysosomes. Cells were examined at random and care was taken to avoid serial sections.

3. Results

3.1. Production and characterisation of NPs

The freeze dried particles, recovered after the encapsulation of INH and MA by the double emulsion evaporation technique, were used in all experiments without further purification. The physical characteristics of the NPs used in the present study are summarized in Table 1. During the manufacture both large (800–900 nm) and small (220–250 nm) particles were formed. Because of the bimodal size distribution nature of the sample the two fractions were separated by varying the centrifugal force, with the larger particles sedimenting at relatively low g-forces as compared to smaller particles that needed relatively high g-forces. Yield for the particles with or without the inclusion of MA was similar. Collected large particles represented 32% whereas the small particles represented 10%. The production yield of the encapsulation process was 42% of particles over the initial solid mass of the reactants. The different NPs were next observed under a SEM. Irrespective of size, the particles were mostly spherical and their surface was generally smooth and uniform (Fig. 1A–D). We observed that the smaller particles had a higher propensity for clumping than the larger ones.

The percentage of encapsulation of the hydrophilic INH was always greater in the particles containing MA (Table 1). This could imply that the addition of MA as a targeting ligand could simultaneously enhance drug loading, and thus the amount that is transferred to infected macrophages. The hydrophobic nature of MA might assist in the reinforcement of the shell around the core containing INH, hence preventing the INH to leak during the particle preparation process. The degree of exposure of the MA on the surface of the NPs was investigated for the large and small NPs by probing them with antibodies present in TB positive patient serum by means of an inhibition ELISA. When MA is exposed on the NPs' surface after incorporation, the MA-NPs will be able to form antibody complexes in solution preventing much of the anti-MA antibodies in human patient serum to bind to immobilized MA on the ELISA plate. This manifested as a reduced ELISA signal (Fig. 1E) when NPs with or without MA were compared in this assay, thus confirming that the PLGA particles display MA as a targeting ligand on the surface.

3.2. Inclusion of mycobacterial cell wall MA into PLGA enhances phagocytic uptake of NPs by macrophages

MA are considered to be one of the major virulence factors of pathogenic mycobacteria. Given their location in the outermost layer of the cell wall, and their ability to bind cholesterol, we investigated whether their inclusion into PLGA would affect phagocytic uptake of NPs by macrophages. For this, BMDM were infected with either *Mtb*, *M. avium* or *M. bovis* BCG and left to incubate for 6 days. The cells were then exposed to PLGA or PLGA/MA particles for 2 h, fixed and processed for electron microscopy.

Qualitative aspects of NP-containing cell profile morphology showed that cells contained significantly more NPs when MA had been included into PLGA (Fig. 2A vs B). Quantitative evaluations showed that 53% of the cell profiles displayed at least one NP when cells had been exposed to PLGA NPs vs 80% of the cell profiles after exposure to PLGA/MA. Evaluation of the average amount of NPs per cell profile showed even clearer differences with a 3 to 4-fold increase when MA was included into the PLGA particles (with MA: 5.4 +/− 0.2 NPs; without MA: 1.5 +/− 0.4 NPs). The histogram distribution clearly showed that after exposure to PLGA NPs for 2 h, more than 70% of the cell profiles displayed either no or only one NPs. In contrast, when MA was included into PLGA, about 70% of the cell profiles displayed 2 or more NPs (Fig. 2C).

These data demonstrated that inclusion of MA into PLGA induced a significantly higher phagocytic uptake of NPs by infected macrophages and, in turn, an increase in the amount of NPs that could potentially transfer active drugs to mycobacterium-containing phagosomes.

3.3. NPs with or without MA are located in phagolysosomes

It is of utmost importance to delineate the exact location of NPs within cells as this will profoundly affect drug transfer to the compartment(s) in which pathogenic mycobacteria reside. Whether they rapidly evade into the cytosol [12,40] or remain enclosed in either immature phagosomes or phagolysosomes [45] is a matter of debate. EM observation of thin sections first showed that NPs, with or without MA, were not free in the macrophage cytosol. They all resided in phagosomes of which the membrane was clearly visible, except for the case of tangential sections through phagosomes for which it is well known that membranes cannot be clearly seen. Evidence for classifying phagosomes as being phagolysosomes or immature phagosomes is based on the luminal presence or absence of electron-dense markers

Table 1
Physical characteristics of NPs prepared by the solvent evaporation freeze drying method.

Preparation	Average particle size (nm)	Poly dispersity index	Zeta potential (mV)	INH and MA loading (w/w)
PLGA/INH	890 (±153)	0.4 (±0.1)	−22.9 (±6.3)	INH: 2%
PLGA/INH/MA	929 (±197)	0.5 (±0.2)	−23.3 (±5.2)	INH: 4% MA: 2%
PLGA/INH	254 (±33)	0.2 (±0.1)	−21.3 (±5.8)	INH: 3%
PLGA/INH/MA	253 (±57)	0.2 (±0.1)	−21.4 (±4.9)	INH: 5% MA: 2%

The (±) indicates the standard deviation (n = 3).

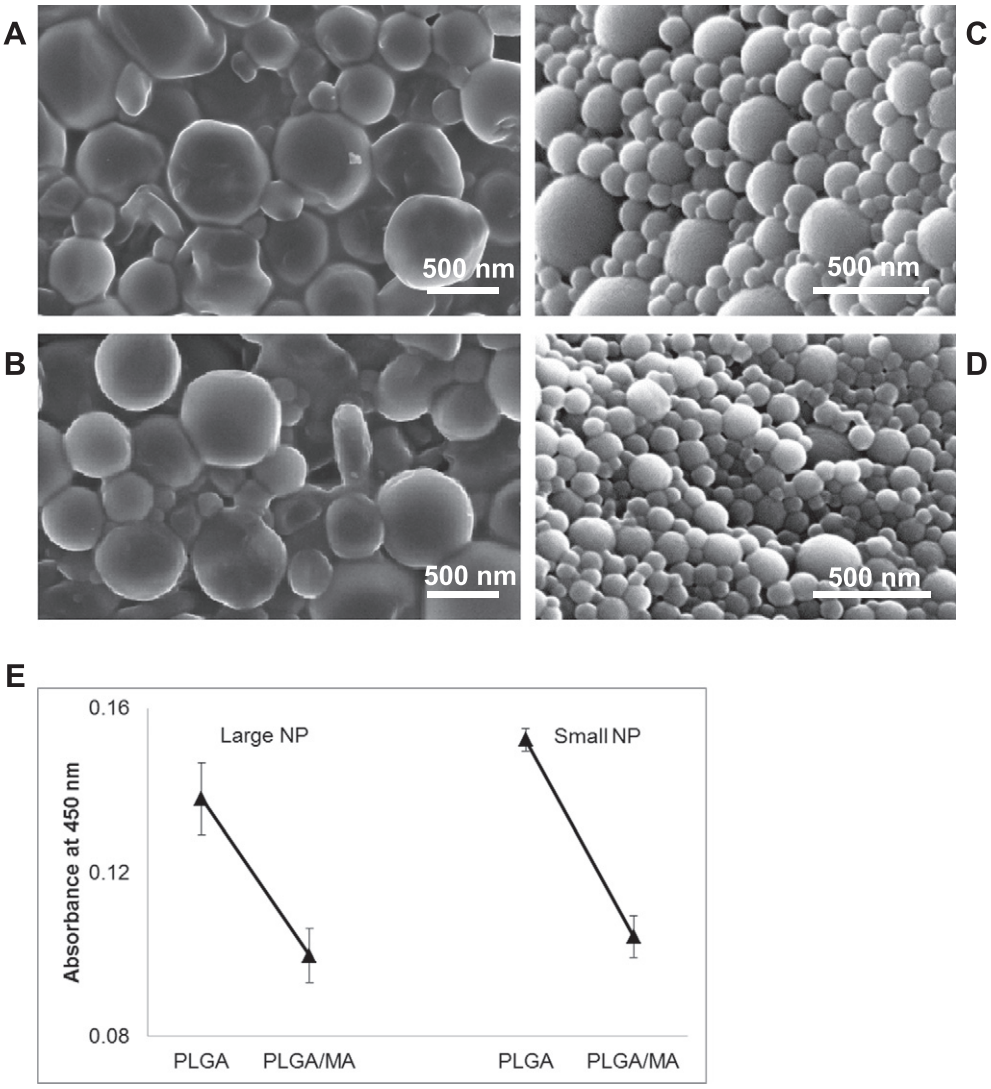

Fig. 1. Morphological appearance of large or small NPs without or with MA incorporated into the PLGA shell. Freeze dried particles, recovered after encapsulation of INH and MA by the double emulsion evaporation technique, were processed for SEM. A) large PLGA particles; B) large PLGA/MA particles; C) small PLGA particles; and D) small PLGA/MA particles. The vast majority of particles are spherical and display a smooth surface. Bars in all panels, 0.5 μm. E) Ability of suspended large and small PLGA/MA particles to inhibit TB patient serum antibody binding to immobilized MA in ELISA. No significant inhibition was detected using a healthy human control serum. The error bars indicate the standard deviation ($n = 3$). Both the large and small MA containing particles are statistically significantly different from particles without MA ($p = 0.05$).

such as BSA-gold (BSA-Au) chased to lysosomes prior to uptake of NPs (Fig. 3A, B, C), or simply based on their electron-dense lysosomal contents (Fig. 3D, E, F) (see e.g., de Chastellier et al., 2009 [54]). To this aim, uninfected cells or cells infected with *M. bovis* BCG were exposed to BSA-Au chased to lysosomes prior to phagocytic uptake of PLGA or PLGA/MA particles. NP-containing phagosomes were observed under the EM for the presence or absence of the lysosomal marker BSA-Au during uptake of NPs (0–4 h uptake). Three different categories of phagosomes were encountered: i) BSA-Au-negative phagosomes containing a single NP. These phagosomes were often surrounded by many BSA-Au-positive lysosomes (Fig. 3A); ii) BSA-Au-positive phagosomes containing a single NP (Fig. 3B) and, iii) BSA-Au-positive phagosomes containing two or more NPs (Fig. 3C). The first category corresponds to an immature phagosome while the two other categories correspond to phagolysosomes that have acquired lysosomal material following their fusion with lysosomes.

NP-containing phagosomes were then scored for the presence or absence of BSA-Au. For both types of NPs, 90 to 100% of the phagosomes containing 2 or more NPs were processed into BSA-Au positive phagolysosomes within a 1-h exposure. In the case of phagosomes containing only one NP, phagosome processing into phagolysosomes was slower. Forty percent of the PLGA/MA-containing phagosomes vs 25% of those containing PLGA NPs also contained the lysosomal marker after a 1-h exposure. This percentage increased with the exposure time in such a way that by 4 h about 78% of the phagosomes with a single NP were BSA-Au positive, qualifying them as phagolysosomes.

Due to the rapid excretion of BSA-Au from BMDM lysosomes (see, e.g. de Chastellier et al., 2006 [27]), it was not possible to use this marker during the chase period. We therefore screened for the presence or absence of the naturally dense lysosomal material which is typical and easy to visualize in BMDM lysosomes and phagolysosomes (see e.g. de Chastellier et al., 2006 [27]). Cells either uninfected or infected with *M. avium*, *M. bovis* BCG or *Mtb* were exposed to PLGA or PLGA/MA particles for 2 h. Cells were washed and re-fed with NP-free medium for up to 9 days. At selected time points during the chase period, NP-containing phagosomes were observed and scored for the presence or absence of dense lysosomal material. Qualitative aspects of NP-containing phagosomes that were positive for dense lysosomal material are shown (Fig. 3D, E, F). Throughout the chase period, 90% of the phagosomes containing either one or more NPs of either type displayed dense lysosomal material and could therefore be classified as being phagolysosomes.

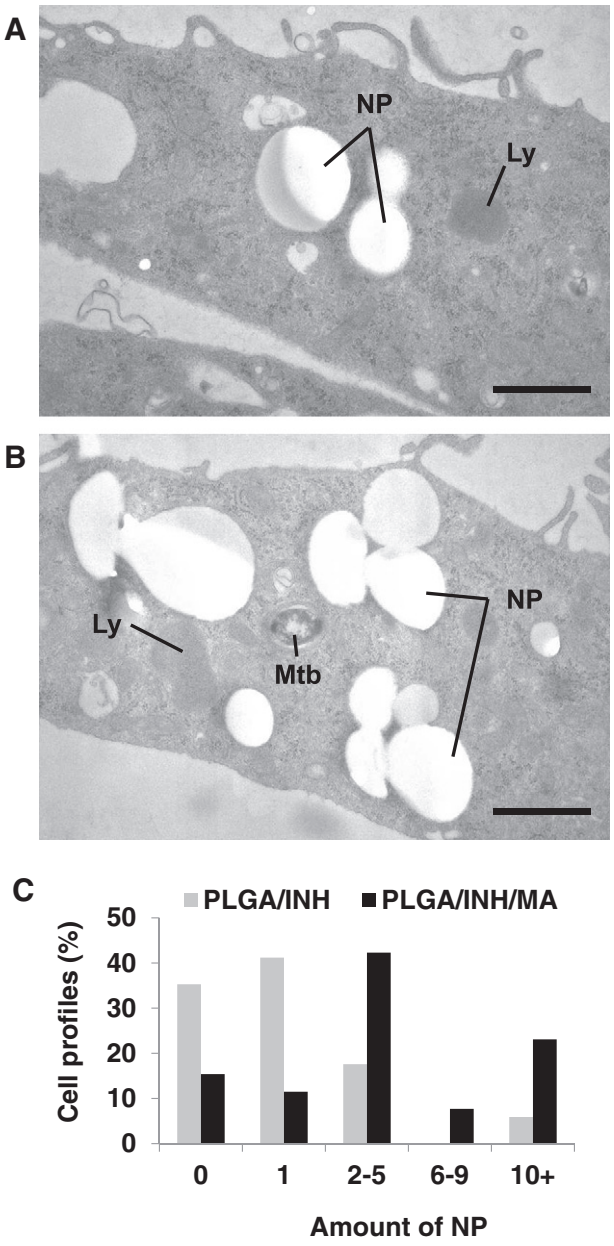

Fig. 2. Inclusion of MA into the PLGA shell enhances phagocytic uptake of particles. BMDM were infected with *Mtb*. At day 6 p.i., cells were exposed to either PLGA NPs or PLGA/MA NPs for 2 h, fixed and processed for TEM. A, B) General views of cell profiles exposed to PLGA NPs (A) or PLGA/MA NPs (B). NPs displayed a similar ultrastructure but were more abundant when MA was incorporated in the PLGA shell. C) Quantitative evaluation of the amount of NPs per cell profile at the same time point. The values shown are accurate to about +/− 12% based on the evaluation of 60 to 100 cell profiles. Ly, lysosomes. Bars in panels A and B: 1 μm.

3.4. Degradation/loss of NPs is a slow process

Mtb treatments make use of free drugs that may be partially or totally degraded as they progress towards the site of infection. Consequently, higher doses and/or longer treatments have been used to avoid transfer of low doses that may induce drug resistance. Nano-encapsulation of first line drugs such as INH is an interesting alternative for circumventing the negative effects of long treatments and/or high doses provided that the polymers used for drug encapsulation resist degradation during progression towards infected cells and are only progressively degraded to deliver the drugs after their internalisation by target cells.

To test NP alteration/degradation and/or secretion from host cells, infected BMDM exposed to PLGA or PLGA/MA particles for 2 h were washed and re-fed with medium devoid of NPs for a period of 0 to 9 days. At selected time points, cells were fixed and processed for EM. NPs were first examined for eventual alterations in shape and size. It is important to note that on thin sections observed under the transmission electron microscope, NPs often display an ellipsoid shape rather than the spherical shape as observed by SEM. This is due to unavoidable sectioning constraints and is not a sign of degradation. At the outset of the chase period, the vast majority of NPs had smooth surfaces (Fig. 4A). During the chase period, blebs appeared on a small fraction of both NP populations (Fig. 4B) and towards the late time points much smaller NPs were found in phagolysosomes (Fig. 4C). A quantitative evaluation of the particle size was performed over a 0 to 5-day chase period. No significant size decrease was observed for PLGA particles. In contrast the size of PLGA/MA particles decreased by 25%. This might be due to the slight amphiphilic nature of MA, which could play the role of additional surfactant that facilitates faster degradation of the NP and loss of MA from the NP surface although one cannot exclude that PLGA might also be damaged by lysosomal enzymes and pH. The percentage of NP-positive cell profiles as well as the average amount of NPs per cell profile was also assessed during the same period of chase. For both PLGA and PLGA/MA, the percentage of NP-positive cells (Fig. 4D) as well as the amount of NPs per cell profile (Fig. 4E) started to decline after 2 days of chase. After 5 days of chase, the mean number of NPs per cell profile remained higher in cells exposed to PLGA/MA than in those exposed to PLGA particles (3.6 and 0.7, respectively), and for both cases, macrophages still contained NPs after a 9-day period of chase (data not shown).

3.5. NPs are targeted to mycobacterium-containing phagolysosomes

We then determined whether PLGA or PLGA/MA NPs reached endomembrane compartments already harbouring different strains of mycobacteria. For this, *M. avium* or *M. bovis* BCG-infected cells were incubated with the NPs that were chased for 0 to 9 days. As expected, NPs were not encountered in phagosomes containing a single mycobacterium and devoid of dense lysosomal material, which correspond to non-matured phagosomes. In contrast, both large and small NPs, with or without MA, were found in some phagolysosomes containing either one or several mycobacteria (Fig. 5A, B, C, D). With the large particles, co-localisation of NPs and mycobacteria occurred starting from day 5 of chase and with a higher frequency when MA had been included in the PLGA polymer. Interestingly, the small NPs were delivered to mycobacterium-containing phagolysosomes much sooner, starting from day 1 of chase.

4. Discussion

The aim of the present work was to design a novel nanoformulation with targeting ligands that would improve efficacy of anti-TB drug delivery. Addition of targeting ligands to the surface of nano drug delivery vehicles have been shown to have beneficial properties such as lowering dosages required and reducing toxic side-effects [7]. Targeting ligands that were studied to date include sugars (for instance mannose), proteins (for example antigens such as peptides), nucleic acid aptamers and antibodies [55–60]. In a fresh approach, we incorporated mycobacterial cell wall MA, a highly hydrophobic molecule, as a targeting ligand into a drug-encapsulating PLGA polymer. MA is an attractive targeting ligand for several reasons. Amongst all targeting candidate ligands considered to date, MA is by far the most robust and stable. This highly hydrophobic molecule could indeed be detected intact in 9000 year old mummified corpses of humans who succumbed to TB [61]. Another important feature of MA is that it is a major virulence factor of pathogenic mycobacteria [19].

Our results showed that the mere inclusion of MA as reagent in the preparation of drug loaded PLGA particles caused them to be exposed on the outer surface of PLGA/MA particles. We also observed a strong

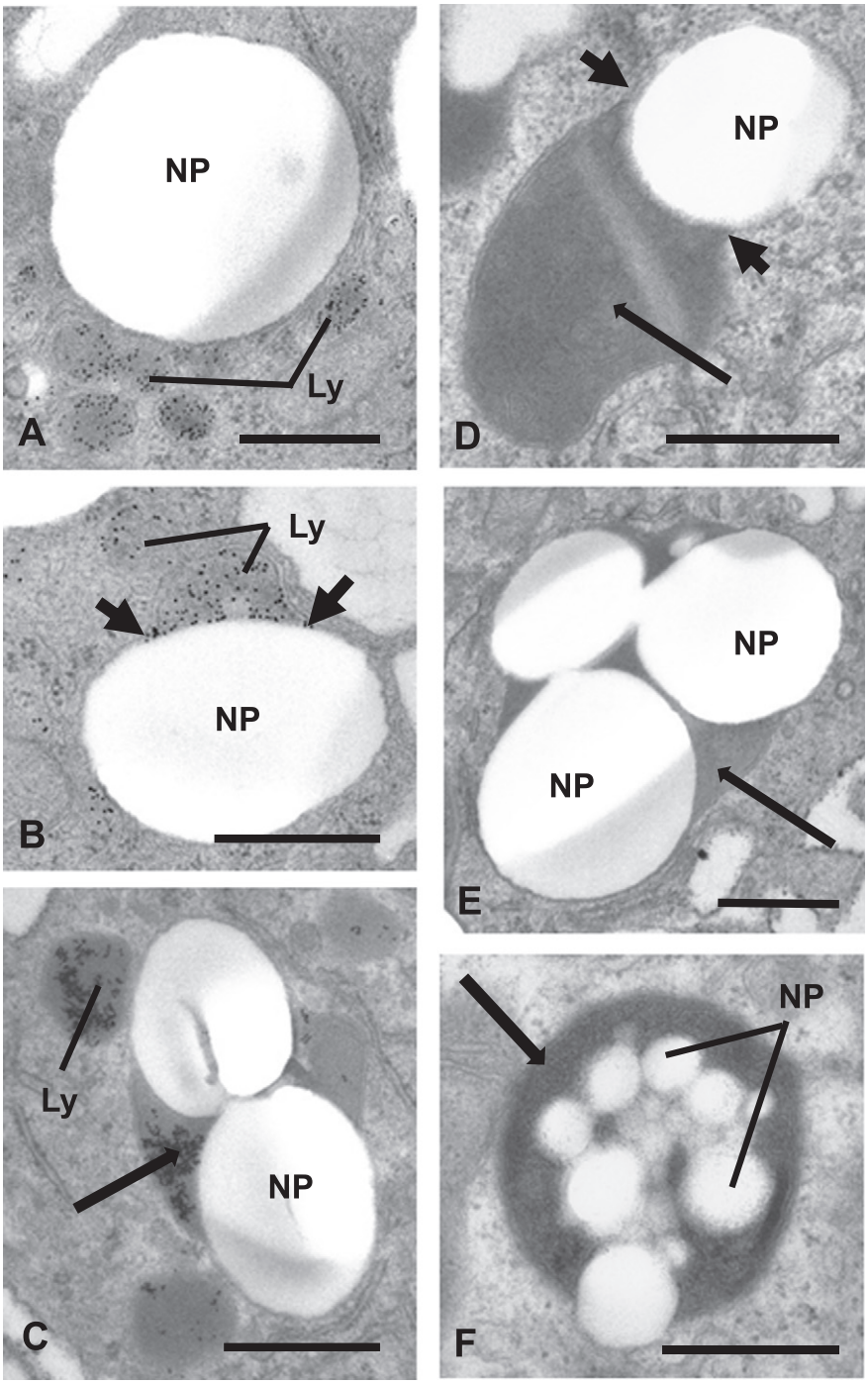

Fig. 3. The preferred residence of PLGA and PLGA/MA particles is a phagolysosome. A, B, C) BMDM were infected with *M. bovis* BCG. At day 6 p.i., cells were exposed to BSA-Au which was chased to lysosomes prior to phagocytic uptake of large PLGA or PLGA/MA particles. A) 2 hr uptake of PLGA NPs. BSA-Au — positive lysosomes (Ly) are located in the close vicinity of a phagosome containing a single NP and no gold particles; B) 2 hr uptake of PLGA/MA. A BSA-Au-positive Ly is fusing (arrowheads) with a phagosome containing a single NP; C) 2 hr uptake of PLGA/MA. This phagosome contains 2 NPs and BSA-Au (arrow), indicating that it has fused with Ly. D, E, F) BMDM were infected with *M. bovis* BCG. Six days later cells were exposed to NPs, fixed and processed for EM. D) 4 hr uptake of large PLGA NPs. The phagosome which contains a single NP is fusing with (arrowheads) a Ly filled with dense material (arrow); E) 4 hr uptake of large PLGA/MA. This phagosome which contains several NPs is filled with dense Ly material (arrow); F) 2 hr uptake of small PLGA/MA followed by a 24-hr chase into NP-free medium. This phagosome which contains several NPs is filled with dense Ly material (arrow). Bars in panels A to F), 0.5 μm.

and significant increase in phagocytic uptake of MA coated NP by mycobacterium-infected macrophages. The facilitation of phagocytic uptake might be best explained by binding of MA-coated NP to cell surface receptors, such as scavenger receptors, involved in phagocytic uptake of *Mtb* [62].

Our data also suggest that tuberculous mycobacterial derived MA can act as anti-TB drug targeting ligand, according to a mechanism of pathogen mimicry. The cholesteroid nature of MA and its ability to bind cholesterol [21] could not only serve as a ligand for cholesterol-rich lipid-raft-like areas on infected cells, or more general cholesterol-rich surfaces associated with granulomas, but may have transformed the NPs to mimic oxidised low density lipoproteins that could be taken up from circulation by macrophages through scavenger receptors. A major consequence of the enhanced phagocytic uptake of NPs coated with MA is that this could in turn lead to a much improved delivery rate and concentration of active drug into the infected cells.

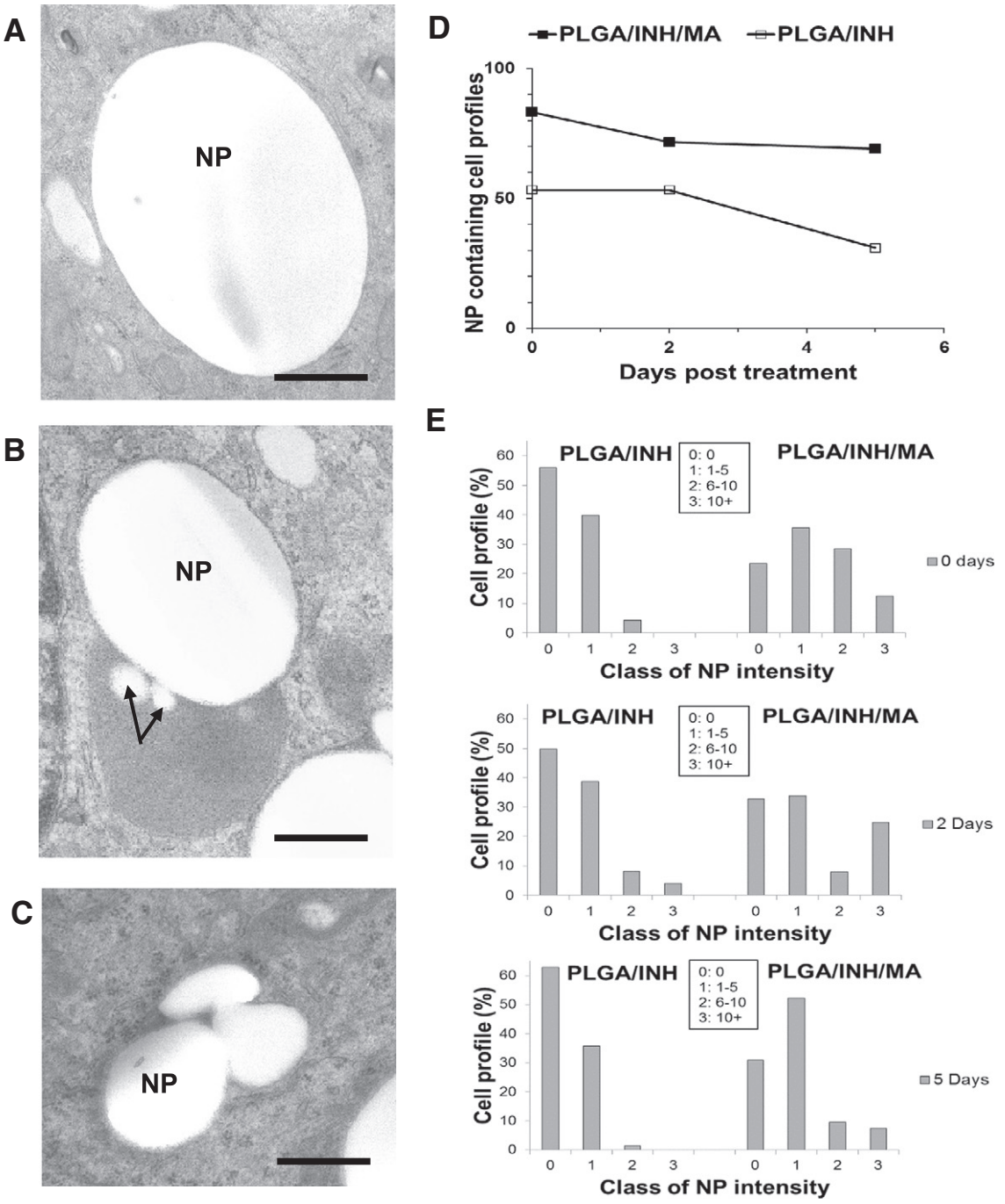

Fig. 4. Degradation/loss of NPs engulfed by BMDM is a slow process. BMDM infected with *M. tuberculosis or M. bovis BCG* were exposed to 800 nm-diameter PLGA or PLGA/MA particles for 2 h and then re-fed with particle-free medium for 0 to 5 days. At selected time points, cells were fixed and processed for TEM. A, B, C) Three major types of particles were seen under the TEM, viz. normal-sized NPs with a smooth surface (A), or with small blebs (arrows) at their surface (B), or NPs for which a significant size decrease was observed (C). D, E) Quantitative evaluation of the percentage of NP-containing cell profiles (D), and of the amount of NPs per cell profile at the same time points. The inserts indicate the number of particles per class of NP intensity (E). The values shown are accurate to about +/− 12% based on the evaluation of 60 to 100 cell profiles. Bars in panels A, B, C), 0.5 μm.

Several studies on NP-driven drug targeting have been aimed at defining the fate of NPs after phagocytic uptake by infected macrophages. Among the different possibilities, localisation in endomembrane compartments, and more especially in phagolysosomes seemed to us the most appropriate. We have, therefore re-investigated this issue with EM approaches. It is important to recall that EM is the only technique that can combine sensitive protein detection methods with detailed information on the ultrastructure of cellular compartments. Contrary to recent information [63], NPs can be easily visualised under the EM provided that the appropriate solvent is used for dehydration steps. We first labelled lysosomes by exposing BMDM to BSA-Au that was chased to lysosomes prior to addition of NPs. At later time points, when BSA-Au had been secreted by macrophages, lysosomes were identified by the presence of electron dense lysosomal material. We concluded that both the MA decorated and non-decorated NPs were localised within phagolysosomes within a few hours after their uptake by macrophages and that they remained in this compartment for at least 9 days. Similarly our small and larger sized non-decorated PLGA NPs resided in the phagolysosomes for up to 9 days in primary murine macrophage cells. Our data definitely put an end to contrasting data presented in the literature for the localisation of unmodified PLGA particles in cells. Panyam et al. reported that differently prepared PLGA particles were able to

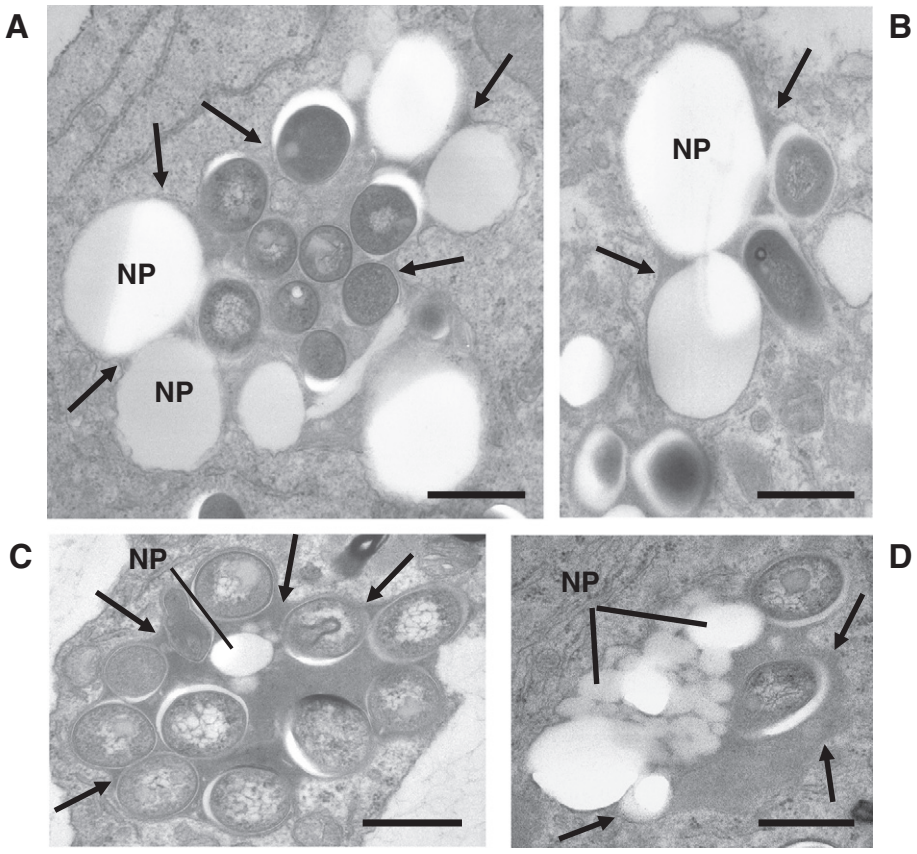

Fig. 5. Both PLGA and PLGA/MA, either large or small, are transferred to mycobacterium-containing phagolysosomes. BMDM infected with either *M. bovis* BCG (A, C, D) or *M. avium* (B) were exposed to PLGA or PLGA/MA for 4 h. At selected time points between 0 and 9 days of chase in NP-free medium, cells were fixed and processed for EM. Thin sections were observed for the presence of NPs within mycobacterium-containing phagosomes. A) exposure to large PLGA NPs, chase for 5 days; B) exposure to large PLGA/MA, chase for 9 days; C) exposure to small PLGA NPs, chase for 6 days; D) exposure to small PLGA/MA, chase for 6 days. In all cases, NPs were found in phagolysosomes containing at least 2 mycobacteria. Arrows point to the phagosome membrane. Bars in panels A, B, C, D), 0.5 μm.

escape the phagosomes into the cytosol [12,40], whereas Kalluru and colleagues in 2013, indicated by means of various techniques, that at least 90% of PLGA particles remained in phagolysosomes after in vitro uptake in BMDM cultures [45].

Clear proof of colocalisation of NPs and mycobacteria in the same macrophages has been recently reported in the zebrafish model [63] but, not of colocalisation in the same cellular compartment. At first glance, this may seem logical, because the vast majority of NPs were found to locate to phagolysosomes, while pathogenic mycobacteria reside and replicate in phagosomes that they prevent from maturing and, as a result, from fusing with lysosomes or phagolysosomes (reviewed in, e.g. de Chastellier, 2009 [34,54]). However, mycobacteria prevent phagosome maturation only when they establish and maintain a close apposition with the phagosome membrane, a phenomenon typically observed with single mycobacterial cell occupation of phagosomes. Whenever several mycobacteria are enclosed in the same phagosome — a frequent event in the case of *M. bovis* BCG or *Mtb*, such phagosomes mature and fuse with lysosomes (reviewed in, e.g., de Chastellier, 2009 [54]). Phagolysosomes with multiple mycobacterial occupation would then also be able to fuse with NP-containing phagolysosomes. As a consequence one may therefore anticipate colocalisation of NPs and mycobacteria. It is important to confirm this, because depending on experimental conditions, such NP-containing phagolysosomes may contain up to 50% or more of the mycobacterial population phagocytosed by macrophages. Our current study gives the first clear proof of drug loaded NPs becoming enclosed within the same phagosomal compartment as the infecting mycobacteria. For both the large and the small NPs, with or without the MA, incidents of colocalisation were observed, but at a higher frequency when MA had been included in the PLGA polymer. Such phagosomes always contained dense lysosomal material, confirming them to be phagolysosomes. The smaller NPs were found to co-localise quicker than the larger particles did.

One major question that arises is whether the drug-loaded NPs have an effect on *M. tuberculosis* or BCG growth and/or degradation. In our previous study [48] human macrophage like cell lines were exposed to MA liganded/unliganded, INH loaded particles for up to two days to confirm antibiotic efficacy. At five hours of incubation, the results of drug efficacy were still found to be variable, but after one or two days of exposure the inhibitory effect of INH was clearly confirmed, also when delivered from MA liganded nanoparticles. In the present study, BMDM cells were exposed to MA liganded/unliganded, INH loaded particles for only two hours, after which the cells were washed and maintained in particle free medium before fixation for EM analysis. This prevented us from observing the efficacy of intracellular INH release, more especially as the particles were shown to degrade very slowly over time which could assist in the slow release of the drug. This corroborated the report by Tracy et al. on in vitro studies done with PLGA microspheres [64], reviewed by Fredenberg in 2011 [65]. The active INH content of the NPs could in future be adjusted to an effective concentration that takes into consideration both the slow drug releasing nature of the PLGA particle and the degree of targetting achievable by the MA ligandation. The concentrations of INH in the particles used for the EM observations were approximately 5 μg/ml in the preparation medium, ten times less than a recent in vitro study of an INH analogue that was tested in PLGA particles [47]. As mentioned before, INH-PLGA NPs have shown sustained drug release over several days in vitro and in vivo [66] and allowed a reduction in treatment frequency in mice and guinea pig models [67–69]. Most chemotherapeutic efficacy studies

in TB on these types of formulations are conducted in vivo, and will be addressed in future work. The in vitro BMDM approach tested here allows better understanding of why targeted anti-TB nanomedicine may work better in vivo.

We propose that the MA-decorated PLGA-based targeted nanotherapeutic, which arguably could be applied both as an inhaled product or an oral formulation, will improve drug delivery at sites of infection to ensure a high localised release of drug, while maintaining low blood levels; thus with minimal toxic side-effects of the drugs. It was previously reported that MA-liganded PLGA particles, intradermally injected into rabbits, caused no measurable degree of inflammation, compared to a Freund's Incomplete Adjuvant control [70]. Combined with a lower dose frequency, this may facilitate the management of the Directly Observed Treatment (DOTs) programme for TB therapy recommended by WHO for global TB control, This is especially relevant for patients with drug resistant TB [71].

With multi- and extensively-drug resistant TB (MDR/XDR-TB) consuming most of the financial resources expended on TB in sub-Saharan Africa [72], the scope provided by the positive indication of MA as targeting ligand for anti-TB nanodrugs may provide timeous hope for a positive solution to a serious current global health threat. These potentially powerful benefits of the targeted nanodrugs could therefore best be trialled in multi-drug resistant TB patients where the issue of toxicity of second line antibiotics treatment is especially prominent.

Acknowledgements

This study was partly funded by the South African Department of Science and Technology, South African National Research Foundation and South African Council for Scientific and Industrial Research. This work was also supported in France by core grants from the Institut National de la Santé et de la Recherche Médicale (INSERM) and the Centre National de la Recherche Scientifique (CNRS) to the Centre d'Immunologie de Marseille-Luminy (CIML) and by grant ANR-09-MIEN-009-03 from the Agence Nationale de la Recherche (French National Research Agency) to CdC.

We thank Irène Caire-Brandli and the members of the electron microscopy core facility of the Institut de Biologie du Développement de Marseille (IBDM) and the CIML for expert technical assistance.

References

[1] WHO, Global Tuberculosis ReportWHO/HTM/TB/2013.11 2013.
[2] F.A. Drobniewski, A.L. Pozniak, A.H. Uttley, Tuberculosis and AIDS, J. Med. Microbiol. 43 (1995) 85–91.
[3] H. McIlleron, G. Meintjes, W.J. Burman, G. Maartens, Complications of antiretroviral therapy in patients with tuberculosis: drug interactions, toxicity, and immune reconstitution inflammatory syndrome, J. Infect. Dis. 196 (2007) S63–S75.
[4] A. Sosnik, A.M. Carcaboso, R.J. Glisoni, M.A. Moretton, D.A. Chiappetta, New old challenges in tuberculosis: potentially effective nanotechnologies in drug delivery, Adv. Drug Deliv. Rev. 62 (2009) 547–559.
[5] WHO, Guidelines for the Programmatic Management of Drug-Resistant TBWHO/HTM/TB/2011.16 2011.
[6] E. Dubnau, J. Chan, C. Raynaud, V.P. Mohan, M.A. Laneelle, K. Yu, A. Quemard, I. Smith, M. Daffe, Oxygenated mycolic acids are necessary for virulence of *Mycobacterium tuberculosis* in mice, Mol. Microbiol. 36 (2000) 630–637.
[7] A. Kumari, S.K. Yadav, S.C. Yadav, Biodegradable polymeric nanoparticles based drug delivery systems, Colloids Surf. B 75 (2010) 1–18.
[8] K.S. Soppimath, T.M. Aminabhavi, A.R. Kulkarni, W.E. Rudzinski, Biodegradable polymeric nanoparticles as drug delivery devices, J. Control. Release 70 (2001) 1–20.
[9] P. Thapa, G. Zhang, C. Xia, A. Gelbard, W.W. Overwijk, C. Liu, P. Hwu, D.Z. Chang, A. Courtney, J.K. Sastry, P.G. Wang, C. Li, D. Zhou, Nanoparticle formulated alpha-galactosylceramide activates NKT cells without inducing anergy, Vaccine 27 (2009) 3484–3488.
[10] K.O. Kisich, S. Gelperina, M.P. Higgins, S. Wilson, E. Shipulo, E. Oganesyan, L. Heifets, Encapsulation of moxifloxacin within poly(butyl cyanoacrylate) nanoparticles enhances efficacy against intracellular *Mycobacterium tuberculosis*, Int. J. Pharm. 345 (2007) 154–162.
[11] B. Semete, L. Booysen, Y. Lemmer, L. Kalombo, L. Katata, J. Verschoor, H.S. Swai, In vivo evaluation of the biodistribution and safety of PLGA nanoparticles as drug delivery systems, Nanomedicine 6 (2010) 662–671.
[12] J. Panyam, V. Labhasetwar, Biodegradable nanoparticles for drug and gene delivery to cells and tissue, Adv. Drug Deliv. Rev. 55 (2003) 329–347.
[13] D. Dube, G.P. Agrawal, S.P. Vyas, Tuberculosis: from molecular pathogenesis to effective drug carrier design, Drug Discov. Today 17 (2012) 760–773.
[14] D.E. Minnikin, Lipids: Complex Lipids, their Chemistry, Biosynthesis and Role, Academic Press, London, UK, 1982.
[15] G. Dobson, D.E. Minnikin, S.M. Minnikin, J.H. Parlett, M. Goodfellow, M. Ridell, M. Magnusson, Systematic analysis of complex mycobacterial lipids, Chemical Methods of Bacterial Systematics, Academic Press, London, 1985.
[16] Y. Fujita, Y. Okamotoa, Y. Uenishib, M. Sunagawab, T. Uchiyamac, I. Yano, Molecular and supra-molecular structure related differences in toxicity and granulomatogenic activity of mycobacterial cord factor in mice, Microb. Pathog. 43 (2007) 10–21.
[17] J. Korf, A. Stoltz, J. Verschoor, P. De Baetselier, J. Grooten, The *Mycobacterium tuberculosis* cell wall component mycolic acid elicits pathogen-associated host innate immune responses, Eur. J. Immunol. 35 (2005) 890–900.
[18] J.E. Korf, G. Pynaert, K. Tournoy, T. Boonefaes, A. van Oosterhout, D. Ginneberge, A. Haegeman, J.A. Verschoor, P. De Baetseller, J. Grooten, Macrophage reprogramming by mycolic acids promotes a tolerogenic response in experimental asthma, Am. J. Respir. Crit. Care Med. 174 (2006) 152–160.
[19] P. Peyron, J. Vaubourgeix, Y. Poquet, F. Levillain, C. Botanch, F. Bardou, M. Daffe', J. Emile, B. Marchou, P. Cardona, C. de Chastellier, F. Altare, Foamy macrophages from tuberculous patients granulomas constitute a nutrient-rich reservoir for *M. tuberculosis* persistence, PLoS Pathog. 4 (2008) e1000204.
[20] J.A. Verschoor, M.S. Baird, J. Grooten, Towards understanding the functional diversity of cell wall mycolic acids of *Mycobacterium tuberculosis*, Prog. Lipid Res. 51 (2012) 325–339.
[21] Y. Benadie, M. Deysel, D.G. Siko, V.V. Roberts, S. Van Wyngaardt, S.T. Thanyani, G. Sekanka, A.M. Ten Bokum, L.A. Collett, J. Grooten, M.S. Baird, J.A. Verschoor, Cholesteroid nature of free mycolic acids from *M. tuberculosis*, Chem. Phys. Lipids 152 (2008) 95–103.
[22] E.V. Beckman, S.A. Porcelli, C.T. Morita, S.M. Behar, S.T. Furlong, M.B. Brenner, Recognition of a lipid antigen by CD1-restricted $\alpha\beta^+$ T cells, Nature 372 (1994) 691–694.
[23] M.A. Goodrum, D.G.R. Siko, T. Niehues, D. Eichelbauer, J.A. Verschoor, Mycolic acids from *Mycobacterium tuberculosis*: purification by countercurrent distribution and T cell stimulation, Microbios 106 (2001) 55–67.
[24] J. Pan, N. Fujiwara, S. Oka, R. Maekura, T. Ogura, L. Yano, Anti-cord factor (trehalose 6,6′-dimycolate) IgG antibody in tuberculosis patients recognizes mycolic acid subclasses, Microbiol. Immunol. 43 (1999) 863–869.
[25] J. Gatfield, J. Pieters, Essential role for cholesterol in entry of mycobacteria into macrophages, Science 288 (2000) 1647–1650.
[26] A. Brzostek, J. Pawelczyk, A. Rumijowska-Galewicz, B. Dziadek, J. Dziadek, *Mycobacterium tuberculosis* is able to accumulate and utilize cholesterol, J. Bacteriol. 191 (2009) 6584–6591.
[27] C. De Chastellier, L. Thilo, Cholesterol depletion in *Mycobacterium avium* — infected macrophages overcome the block in phagosome maturation and leads to the reversible sequestration of viable mycobacteria in phagolysosome derived autophagic vacuoles, Cell. Microbiol. 8 (2006) 242–256.
[28] Y. Lemmer, S.T. Thanyani, P.J. Vrey, C.H.S. Driver, L. Venter, S. van Wyngaardt, A.M.C. ten Bokum, K.I. Ozoemena, L.A. Pilcher, D.G. Fernig, A.C. Stoltz, H.S. Swai, J.A. Verschoor, Detection of antimycolic acid antibodies by liposomal biosensors, Methods Enzymol. 464 (2009) 80–102.
[29] C. de Chastellier, F. Forquet, A. Gordon, L. Thilo, Mycobacterium requires an all-around closely apposing phagosome membrane to maintain the maturation block and this apposition is re-established when it rescues itself from phagolysosomes, Cell. Microbiol. 11 (2009) 1190–1207.
[30] J.A. Armstrong, P. D'arcy Hart, Phagosome–lysosome interactions in cultured macrophages infected with virulent tubercle bacilli, J. Exp. Med. 142 (1975) 1–15.
[31] C. Frehel, C. de Chastellier, T. Lang, N. Rastogi, Evidence for inhibition of fusion of lysosomal and prelysosomal compartments with phagosomes in macrophages infected with pathogenic *Mycobacterium avium*, Infect. Immun. 52 (1986) 252–262.
[32] C. De Chastellier, T. Lang, L. Thilo, Phagocytic processing of the macrophage endoparasite, *Mycobacterium avium*, in comparison to phagosomes which contain *Bacillus subtilis* or latex beads, Eur. J. Cell Biol. 68 (1995) 167–182.
[33] C. De Chastellier, L. Thilo, Phagosome maturation and fusion with lysosomes in relation to surface property and size of the phagocytic particle, Eur. J. Cell Biol. 74 (1997) 49–62.
[34] R. Pietersen, L. Thilo, C. de Chastellier, *Mycobacterium tuberculosis* and *Mycobacterium avium* modify the composition of the phagosomal membrane in infected macrophages by selective depletion of cell surface derived glycoconjugates, Eur. J. Cell Biol. 83 (2004) 153–158.
[35] D.L. Clemens, M.A. Horwitz, Characterization of the *Mycobacterium tuberculosis* phagosome and evidence that phagosomal maturation is inhibited, J. Exp. Med. 181 (1995) 257–270.
[36] Q.N. Myrvik, E.S. Leake, M.J. Wright, Disruption of phagosomal membranes of normal alveolar macrophages by the H37Rv strain of *Mycobacterium tuberculosis*. A correlate of virulence, Am. Rev. Respir. Dis. 129 (1984) 322–328.
[37] K.A. McDonough, Y. Kress, B.R. Bloom, Pathogenesis of tuberculosis: interaction of *Mycobacterium tuberculosis* with macrophages, Infect. Immun. 61 (1993) 2763–2773.
[38] N. van der Wel, D. Hava, D. Houben, D. Fluitsma, M. van Zon, J. Pierson, M. Brenner, P.J. Peters, *M. tuberculosis* and *M. leprae* translocate from the phagolysosome to the cytosol in myeloid cells, Cell 129 (2007) 1287–1298.
[39] B.Y. Lee, D.L. Clemens, M.A. Horwitz, The metabolic activity of *Mycobacterium tuberculosis*, assessed by use of a novel inducible GFP expression system, correlates with its capacity to inhibit phagosomal maturation and acidification in human macrophages, Mol. Microbiol. 68 (2008) 1047–1060.

[40] J. Panyam, W. Zhou, S. Prabha, S.K. Sahoo, V. Labhasetwar, Rapid endo-lysosomal escape of poly(DL-lactide-coglycolide) nanoparticles: implications for drug and gene delivery, FASEB J. 16 (2002) 1217–1226.
[41] A.J. Gomes, A.S. Faustino, A.E. Machado, M.E. Zaniquelli, T. de Paula Rigoletto, C.N. Lunardi, L.O. Lunardi, Characterization of PLGA microparticles as a drug carrier for 3-ethoxycarbonyl-2 h-benzofuro[3,2-f]-1-benzopyran-2-one. Ultrastructural study of cellular uptake and intracellular distribution, Drug Deliv. 13 (2006) 447–454.
[42] F.Y. Cheng, S.P. Wang, C.H. Su, T.L. Tsai, P.C. Wu, D.B. Shieh, J.H. Chen, P.C. Hsieh, C.S. Yeh, Stabilizer-free poly(lactide-co-glycolide) nanoparticles for multimodal biomedical probes, Biomaterials 29 (2008) 2104–2112.
[43] M.S. Cartiera, K.M. Johnson, V. Rajendran, M.J. Caplan, W.M. Saltzman, The uptake and intracellular fate of PLGA nanoparticles in epithelial cells, Biomaterials 30 (2009) 2790–2798.
[44] C. Schliehe, C. Schliehe, M. Thiry, U.I. Tromsdorf, J. Hentschel, H. Weller, M. Groettrup, Microencapsulation of inorganic nanocrystals into PLGA microsphere vaccines enables their intracellular localization in dendritic cells by electron and fluorescence microscopy, J. Control. Release 151 (2011) 278–285.
[45] R. Kalluru, F. Fenaroli, D. Westmoreland, L. Ulanova, A. Maleki, N. Roos, M. Paulsen Madsen, G. Koster, W. Egge-Jacobsen, S. Wilson, H. Roberg-Larsen, G.K. Khuller, A. Singh, B. Nyström, G. Griffiths, Poly(lactide-co-glycolide)-rifampicin nanoparticles efficiently clear *Mycobacterium bovis* BCG infection in macrophages and remain membrane-bound in phago-lysosomes, J. Cell Sci. 126 (2013) 3043–3054.
[46] T. Onoshita, Y. Shimizu, N. Yamaya, M. Miyazaki, M. Yokoyama, N. Fujiwara, T. Nakajima, K. Makino, H. Terada, M. Haga, The behavior of PLGA microspheres containing rifampicin in alveolar macrophages, Colloids Surf. B: Biointerfaces 76 (2010) 151–157.
[47] T.J. de Faria, M. Roman, N.M. de Souza, R. De Vecchi, J.V. de Assis, A.L. dos Santos, H. Bechtold, N. Winter, M.J. Soares, L.P. Silva, M.V. De Almeida, A. Báfica, An isoniazid analogue promotes *Mycobacterium tuberculosis*—nanoparticle interactions and enhances bacterial killing by macrophages, Antimicrob. Agents Chemother. 56 (2012) 2259–2267.
[48] Y. Lemmer, Assessment of Mycolic Acids as Ligand for Nanoencapsulated Antituberculosis Drug Targeting, Department Biochemistry, University of Pretoria 2010, pp. 1–190.
[49] A. Lamprecht, N. Ubrich, M. Hombreiro Perez, C.-M. Lehr, M. Hoffman, P. Maincent, Biodegradable monodispersed nanoparticles prepared by pressure homogenization-emulsification, Int. J. Pharm. 184 (1999) 97–105.
[50] M.S. Hora, R.K. Rana, J.H. Nunberg, T.R. Tice, R.M. Gilley, M.E. Hudson, Release of human serum albumin from poly(lactide-co-glycolide) microspheres, Pharm. Res. 7 (1990) 1190–1194.
[51] S.P.S. Khanuja, S. Srivastava, T.R.S. Kumar, A.K. Shasany, M.P. Darokar, S. Awasthi, PCT WO 03/080860. A Quick and Sensitive Method of Quantifying Mycolic Acid, in: W.I.P. Organisation (Ed.), 2003.
[52] S.T. Thanyani, V. Roberts, D.G. Siko, P. Vrey, J.A. Verschoor, A novel application of affinity biosensor technology to detect antibodies to mycolic acid in tuberculosis patients, J. Immunol. Methods 332 (2008) 61–72.
[53] M. Beukes, Y. Lemmer, M. Deysel, J.R. Al Dulayymi, M. Baird, G. Koza, M.M. Iglesias, R.R. Rowles, C. Theunissen, J. Grooten, G. Toschi, V.V. Roberts, L. Pilcher, S. Van Wyngaardt, N. Mathebula, M. Balogun, A.C. Stoltz, J.A. Verschoor, Structure–function relationships of the antigenicity of mycolic acids in tuberculosis patients, Chem. Phys. Lipids (2010) http://dx.doi.org/10.1016/j.chemphyslip.2010.1009.1006.
[54] C. De Chastellier, The many niches and strategies used by pathogenic mycobacteria for survival within host macrophages, Immunobiology 214 (2009) 526–542.
[55] F. Alexis, E. Pridgen, L.K. Molnar, O.C. Farokhzad, Factors affecting the clearance and biodistribution of polymeric nanoparticles, Mol. Pharm. 5 (2008) 505–515.
[56] K. Ohashi, T. Kabasawa, T. Ozeki, H. Okada, One-step preparation of rifampicin/poly(lactic-co-glycolic acid) nanoparticle-containing mannitol microspheres using a four-fluid nozzle spray drier for inhalation therapy of tuberculosis, J. Control. Release 135 (2009) 19–24.
[57] P.V. Kumar, A. Asthana, T. Dutta, N.K. Jain, Intracellular macrophage uptake of rifampicin loaded mannosylated dendrimers, J. Drug Target. 14 (2006) 546–556.
[58] J. Cheng, B.A. Teply, I. Sherifi, J. Sung, G. Luther, F.X. Gu, E. Levy-Nissenbaum, A.F. Radovic-Moreno, R. Langer, O.C. Farokhzad, Formulation of functionalized PLGA-PEG nanoparticles for in vivo targeted drug delivery, Biomaterials 28 (2007) 869–876.
[59] X. Montet, R. Weissleder, L. Josephson, Imaging pancreatic cancer with a peptide-nanoparticle conjugate targeted to normal pancreas, Bioconjug. Chem. 17 (2006) 905–911.
[60] F. Shamsipour, A.H. Zarnani, R. Ghods, M. Chamankhah, F. Forouzesh, S. Vafaei, A.A. Bayat, M.M. Akhondi, M. Ali Oghabian, M. Jeddi-Tehrani, Conjugation of monoclonal antibodies to super paramagnetic iron oxide nanoparticles for detection of HER2/neu antigen on breast cancer cell lines, Avicenna J. Med. Biotechnol. 1 (2009) 27–31.
[61] I. Hershkovitz, H.D. Donoghue, D.E. Minnikin, G.S. Besra, O.Y.-C. Lee, A.M. Gernaey, E. Galili, V. Eshed, C.L. Greenblatt, E. Lemma, G.K. Bar-Gal, M. Spigelman, Detection and molecular characterization of 9000-year-old *Mycobacterium tuberculosis* from a Neolithic settlement in the Eastern Mediterranean, PLoS ONE 3 (2008) e3426.
[62] S. Zimmerli, S. Edwards, J.D. Ernst, Selective receptor blockade during phagocytosis does not alter the survival and growth of *Mycobacterium tuberculosis* in human macrophages, Am. J. Respir. Cell Mol. Biol. 15 (1996) 760–770.
[63] F. Fenaroli, D. Westmoreland, J. Benjaminsen, T. Kolstad, F.M. Skjeldal, A.H. Meijer, M. van der Vaart, L. Ulanova, N. Roos, B. Nyström, J. Hildahl, G. Griffiths, Nanoparticles as drug delivery system against tuberculosis in zebrafish embryos: direct visualization and treatment, ACS Nano 8 (2014) 7014–7026.
[64] M.A. Tracy, K.L. Ward, L. Firouzabadian, Y. Wang, N. Dong, R. Qian, Y. Zhang, Factors affecting the degradation rate of poly(lactide-co-glycolide) microspheres in vivo and in vitro, Biomaterials 20 (1999) 1057–1062.
[65] S. Fredenberg, M. Wahlgren, M. Reslow, A. Axelsson, The mechanisms of drug release in poly(lactic-co-glycolic acid)-based drug delivery systems—a review, Int. J. Pharm. 415 (2011) 34–52.
[66] M. Dutt, G.K. Khuller, Liposomes and PLG microparticles as sustained release antitubercular drug carriers — an in vitro-in vivo study, Int. J. Antimicrob. Agents 18 (2001) 245–252.
[67] C.M. Johnson, R. Pandey, S. Sharma, G.K. Khuller, R.J. Basaraba, I.M. Orme, A.J. Lenaerts, Oral therapy using nanoparticle-encapsulated antituberculosis drugs in guinea pigs infected with *Mycobacterium tuberculosis*, Antimicrob. Agents Chemother. 49 (2003) 4335–4338.
[68] A. Sharma, R. Pandey, S. Sharma, G.K. Khuller, Chemotherapeutic efficacy of poly (DL-lactide-co-glycolide) nanoparticle encapsulated antitubercular drugs at sub-therapeutic dose against experimental tuberculosis, Int. J. Antimicrob. Agents 24 (2004) 599–604.
[69] R. Pandey, A. Zahoor, S. Sharma, G.K. Khuller, Nanoparticle encapsulated antitubercular drugs as a potential oral drug delivery system against murine tuberculosis, Tuberculosis 83 (2003) 373–378.
[70] H. Ranchod, Chemically Synthetic Mycolic Acids as Vaccine Adjuvants, Department Biochemistry, University of Pretoria 2014, pp. 1–83.
[71] A.D. Calver, A.A. Falmer, M. Murray, O.J. Strauss, E.M. Streicher, M. Hanekom, T. Liversage, M. Masibi, P.D. van Helden, R.M. Warren, T.C. Victor, Emergence of increased resistance and extensively drug-resistant tuberculosis despite treatment adherence, South Africa, Emerg. Infect. Dis. 16 (2010) 264–271.
[72] P.R. Donald, P.D. van Helden, The global burden of tuberculosis—combating drug resistance in difficult times, N. Engl. J. Med. 4 (2009) 2393–2395.